Quaternary Research 82 (2014) 132–145

Contents lists available at ScienceDirect

Quaternary Research

journal homepage: www.elsevier.com/locate/yqres

Glacial and Holocene terrestrial temperature variability in subtropical east Australia as inferred from branched GDGT distributions in a sediment core from Lake McKenzie

Martijn Woltering [a,*,1], Pia Atahan [b], Kliti Grice [a], Henk Heijnis [b], Kathryn Taffs [c], John Dodson [b]

[a] WA-Organic and Isotope Geochemistry Centre, Department of Chemistry, Curtin University, Perth, WA, Australia
[b] Institute for Environmental Research, Australian Nuclear Science and Technology Organisation, Sydney, PMB 1 Menai NSW 2234, Australia
[c] Southern Cross Geoscience and School of Environment, Science and Engineering, Southern Cross University, PO Box 157, Lismore NSW 2480, Australia

ARTICLE INFO

Article history:
Received 12 July 2013
Available online 18 March 2014

Keywords:
Temperature reconstruction
Australia
Subtropical
Temperature proxy
Branched GDGT
Palaeolimnology
Lake
Fraser Island
Holocene
Last Glacial Maximum

ABSTRACT

Branched glycerol dialkyl glycerol tetraether (GDGT) distributions observed in a sediment core from Lake McKenzie were utilized to quantitatively reconstruct the pattern of mean annual air temperature (MAAT) from coastal subtropical eastern Australia between 37 and 18.3 cal ka BP and 14.0 cal ka BP to present. Both the reconstructed trend and amplitude of MAAT changes from the top of the sediment core were nearly identical to a local instrumental MAAT record from Fraser Island, providing confidence that in this sediment core branched GDGTs could be used to produce a quantitative record of past MAAT. The reconstructed trend of MAAT during 37 to 18.3 cal ka BP and timing of the Last Glacial Maximum (LGM) in the Lake McKenzie record were in agreement with previously published nearby marine climate records. The amplitude of lower-than-present MAAT during the LGM potentially provides information on the latitude of separation of the Tasman Front from the East Australian current in the subtropical western Pacific. The Lake McKenzie record shows an earlier onset of near modern day warm temperatures in the early Holocene compared to marine records and the presence of a warmer than present day period during the mid-Holocene.

Introduction

Continental climate dynamics in Australia over the last 35,000 years are poorly understood. This is in part the result of a paucity of long, quantitative and well dated climate reconstructions distributed over this continent (Reeves et al., 2013). Most of the information about the thermal history of Australia comes from sea surface temperature reconstructions from marine archives, from palynological reconstruction studies and from amino acid racemisation studies of emu eggs (Reeves et al., 2013, and references therein). Although these methods have provided valuable insights on continental climate in Australia, there are issues concerning the independence, resolution and quantitative nature of these kinds of temperature reconstructions (Webb, 1986; Kershaw and Nanson, 1993; Miller et al., 1997; Moss and Kershaw, 2000; Pickett et al., 2004).

A potential and relatively novel way to obtain prospective independent temperature information from the continents is based on the relative distribution of glycerol dialkyl glycerol tetraether (GDGT) lipids observed in lacustrine sediment archives. Branched GDGTs are a set of core membrane lipids with sn-1, 2 stereochemistry and basic *n*-alkyl chains, with varying numbers of methyl branches and cyclopentane moieties (Sinninghe Damsté et al., 2000; Weijers et al., 2006). The specific sn-1, 2 stereochemistry suggests a bacterial origin of these lipids (Weijers et al., 2006), although the specific bacterial source of all of the branched GDGT is yet to be identified. A relationship between branched GDGT distributions and temperature was first identified in a globally distributed soil sample set studied by Weijers et al. (2007b) and leads to the introduction of the methylation index of branched tetraethers (MBT) and the cyclisation ratio of branched tetraethers (CBT) that together could be used as a proxy to infer past continental temperatures based on the branched GDGT distributions in a given sample. The MBT/CBT index from terrestrial soils has subsequently been used to estimate paleotemperatures in marine sediment cores from coastal regions (Weijers et al., 2007a; Rueda et al., 2009), and can potentially be used to reconstruct palaeotemperature from lacustrine sediment cores (e.g. Tierney et al., 2010; Niemann et al., 2012).

Although many studies observed that branched GDGTs are ubiquitously found in lake sediments (e.g. Sinninghe Damsté et al., 2009; Tierney et al., 2010; Tyler et al., 2010; Niemann et al., 2012), numerous studies have found evidence suggesting that branched GDGTs in many lake sediments were not only derived from the surrounding soils.

* Corresponding author.
E-mail address: Martijn.Woltering@csiro.au (M. Woltering).
[1] Current address: CSIRO Earth Science and Resource Engineering, Australian Resources Research Centre, Kensington, Perth WA 6151 Australia.

http://dx.doi.org/10.1016/j.yqres.2014.02.005
0033-5894/

Instead, at least some of the branched GDGTs appear to have been produced within the water column or sediments of these lakes (Sinninghe Damsté et al., 2009; Tierney and Russell, 2009; Bechtel et al., 2010; Loomis et al., 2011; Tierney et al., 2012). In these lakes with in situ branched GDGT production the application of the soil calibration by Weijers et al. (2007a) consistently resulted in temperature estimates that were weakly correlated, and uniformly lower, than instrumental records of water or nearby air temperatures. Regional and global lake calibrations (e.g. Pearson et al., 2011; Sun et al., 2011; Loomis et al., 2012) are currently available that may be better suited to inferring temperatures from lake sediments where in situ production of branched GDGTs is apparent. Several studies have used branched GDGT distributions in lake sediments to produce temperature reconstructions (Tyler et al., 2010; Fawcett et al., 2011; Das et al., 2012; Loomis et al., 2012; Niemann et al., 2012; Sinninghe Damsté et al., 2012). In some of these studies it was observed that the reconstructed temperature trends (Niemann et al., 2012; Loomis et al., 2012; Das et al., 2012) showed a certain degree of agreement with other palaeoenvironmental reconstructions or instrumental temperature records. This demonstrates the potential of using branched GDGT distributions in lake sediments as a proxy for paleotemperature. However, in other studies like Sinninghe Damsté et al. (2012) and Tyler et al. (2010), reconstructed temperature trends did not appear to match any proxy or instrumental temperature record indicating that the successful application of this proxy is still relatively poorly understood.

Here we report the results of a study that determined branched GDGT distributions in a dated sediment core from Lake McKenzie on Fraser Island in subtropical Eastern Australia. Based on a comparison with a local instrumental temperature record it was assessed whether branched GDGT distributions could be used as a paleotemperature proxy. Subsequently, a reconstruction of the trend and amplitude of temperature changes was produced for this subtropical eastern Australian site, which covered both the end of the last Glacial and Holocene periods. The produced Lake McKenzie temperature record was subsequently compared to other paleoclimate records and interpreted in a paleoclimate perspective.

Materials and methods

Site location and sampling description

Lake McKenzie (25°26′51″S, 153°03′12″E, 90 m asl) is a perched oligotrophic lake, located on Fraser Island (Fig. 1). The lake is ca. 1200 m long and up to ca. 930 m wide and has a depth up to 8.5 m. Lake McKenzie formed in a depression created by the wind, when organic matter, such as leaves, bark, and dead plants, gradually built up and hardened creating an impermeable base layer of cemented organic matter (Longmore, 1997). Rainfall accumulated in the depression creating a lake. Lake McKenzie sits above the regional aquifer and does not have an inflow or outflow creek and therefore can be considered to be a hydrologically closed basin (IUCN, 1992), making the lake level highly susceptible to changes in precipitation and evaporation. The water of Lake McKenzie is acidic, with a pH of 3.7–4.8 (Hadwen, 2002) due to input from organic acids produced by decaying organic matter. The soils surrounding Lake McKenzie are rapidly draining aeric podosols that consist of aeolian siliceous sands that show low soil development and low nutrient availability (McKenzie et al., 2004).

Two adjacent sediment cores were extracted from the centre of the deepest basin of Lake McKenzie in 2010, in ca. 8.3 m water depth. The cores (LM1 and LM2) were extracted using a gravity corer, extruded on the lake edge, and sliced into either 0.25 cm thick (LM1) or 1 cm thick (LM2) samples. Total un-extruded core length was measured at regular intervals during sampling to monitor loss of core length. Samples were placed in individual plastic zip-lock bags before being transported and stored in laboratory freezers.

In addition to sampling of a sediment core from Lake McKenzie, soil samples (top 10 cm) were collected from three locations in the drainage basin (Fig. 1) in May 2012. These samples were stored in zip-lock bags for transport and storage in a laboratory freezer before extraction and analyses.

Age model based on ^{210}Pb and ^{14}C AMS dates

The age model of core LM2 is based on twelve ^{14}C AMS and five ^{210}Pb ages. With the exception of one large wood fragment recovered from core LM1, terrestrial plant macrofossils, such as leaves or seeds, were not encountered in either sediment cores. For this reason pollen concentrates were prepared for AMS ^{14}C dating. Physical and chemical pre-treatment of Lake McKenzie samples were conducted prior to AMS ^{14}C measurement with the purpose of isolating pollen and removing contaminants. Samples were sieved to collect a 10–150 μm size fraction, separated by heavy liquid flotation (LST; SG = 1.8) and treated with NaOH (10%), HCl (10%) and H_2SO_4 (98%). Pre-treatment of the wood fragment followed the standard acid–alkali–acid method used at the Australian Nuclear Science and Technology Organisation (ANSTO) (Hua et al., 2004). Radiocarbon dates were calibrated using

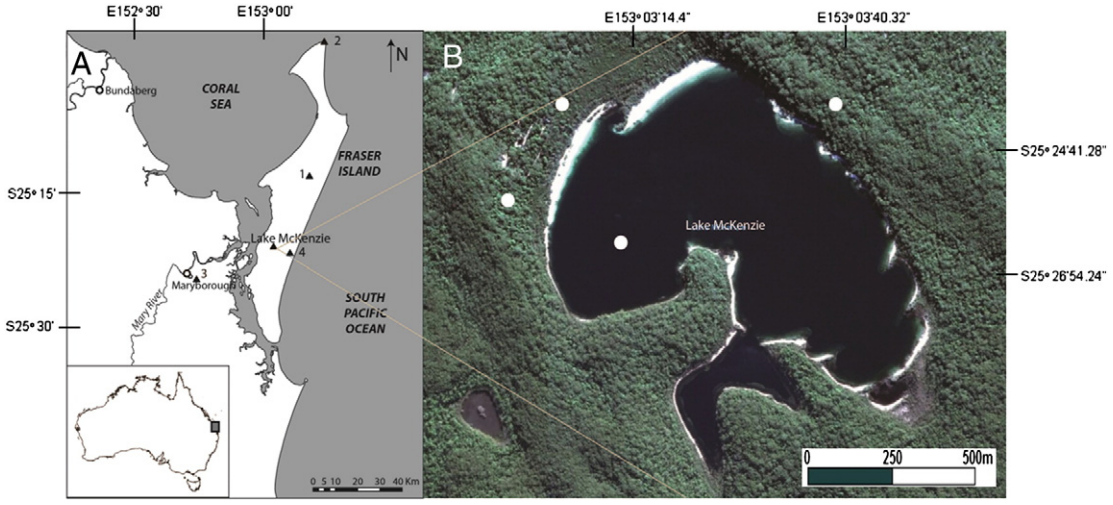

Figure 1. A: Map showing the location of Fraser Island and Lake McKenzie. The black triangle (1) marks the locations of a previous palaeoenvironmental study on Fraser Island at Lake Allom; (2) Sandy Cape Lighthouse weather station; (3) Maryborough weather station and (4) Eurong weather station. B: White circles mark the location of cores LM1 and LM2 within Lake McKenzie and locations of soil samples surrounding the lake.
Google Earth version 6.2 software, 2012.

https://doi.org/10.1016/j.yqres.2014.02.005 Published online by Cambridge University Press

the INTCAL 09 calibration curve (Reimer et al., 2009). Calibrated ages in the paper are reported relative to present (1950 CE) and are followed by a 'cal ka BP' post-fix. Single dates mentioned in the paper refer to the median age in the 2σ calibrated age range.

Abundance of atmosphere-derived ^{210}Pb ($^{210}Pb_{unsupported}$) in the upper sediment was used to estimate recent sediment accumulation rates at Lake McKenzie. The method, which has been described in detail by Appleby and Oldfield (1978), Appleby and Oldfield (1992) and Appleby (2001), uses down-core change in $^{210}Pb_{unsupported}$ activity to calculate an accumulation rate based on the ^{210}Pb half-life of 22.26 ± 0.22 yr. $^{210}Pb_{unsupported}$ was estimated by subtracting activity of supported ^{210}Pb ($^{210}Pb_{supported}$), derived from in situ decay of Radium-226 (^{226}Ra), from total ^{210}Pb ($^{210}Pb_{total}$) activity, which was measured indirectly from its progeny polonium-210 (^{210}Po). $^{210}Pb_{supported}$ was measured indirectly from its grandparent radioisotope ^{226}Ra. Both the CIC (constant initial concentration) and the CRS (constant rate of supply) models (Appleby and Oldfield, 1978; Appleby, 2001) were used to calculate calendar ages.

$^{210}Pb_{supported}$ and $^{210}Pb_{total}$ were measured in the upper 8.5 cm of core LM1. Between 0.18 and 1.23 g of sediment, the samples were prepared by heating in HNO_3 at 60°C. Once evaporated, small amounts of H_2O_2 (10%) were added with heating until the reaction subsided. The samples were evaporated again before refluxing in a mixture of HNO_3 and HCl (1:3; 50–60°C) for at least 4 h. Samples were subsequently redissolved in HCl (6 M) and centrifuged to separate the supernatant from the residue. The residue was washed and discarded. The supernatant and the residue wash were collected and processed to remove excess iron by diethyl ether solvent extraction. The recovery of the preparation method was assessed using radioactive tracers ^{133}Ba (~85 Bq) for ^{226}Ra recovery and ^{209}Po (~0.2 Bq) for ^{210}Po recovery, which were added at the start of the sample processing procedure. ^{210}Po and ^{209}Po were isolated by auto-deposition onto silver discs using $NH_2OH \cdot HCl$, and then analysed with ORTEC alpha spectrometers. ^{226}Ra and ^{133}Ba were isolated by co-precipitation and collected as colloidal micro-precipitates on 0.1 μm Millipore VV membrane filters. ^{133}Ba was analysed using a HPGE gamma spectrometer and ^{226}Ra was analysed using ORTEC alpha spectrometers.

Total organic carbon (%TOC)

All samples from core LM1 and LM2 were treated with HCl (10%) to remove carbonates before analysis on a Flash 2000 HT Elemental Analyser for TOC%.

GDGT lipid extraction and analysis

All sediment and soil samples were freeze dried before extraction commenced. About 1–5 g of sediment and ~35 grams of soil sample was extracted using a Dionex accelerated solvent extractor (ASE) 200 system using a 9:1 v:v dichloromethane (DCM): methanol (MeOH) mixture. Total lipid extracts were separated into non-polar and polar fractions over a small Al_2O_3 column in a pasteur pipette, using hexane: DCM (9:1, v:v) and DCM: MeOH (1:1, v:v) as eluents (Schouten et al., 2007). The polar fraction containing the GDGTs was dried, redissolved in hexane: isopropanol (99:1, v:v) and filtered with a 0.45 μm filter. High performance liquid chromatography–atmospheric pressure chemical ionization–mass spectrometry (HPLC–APCI–MS) analysis was carried out on a Thermo Oribtrap XL LC/MSD using scan window of (1015–1305 *m/z*). For data analysis different 0.1 amu scan windows were created for crenarchaeol (IV, *m/z* 1292.2), and the nine different branched GDGTs III, *m/z* 1050; IIIb, *m/z* 1048; IIIc, *m/z* 1046; II, *m/z* 1036; IIb, *m/z* 1034; IIc, *m/z* 1032; I, *m/z* 1022; Ib, *m/z* 1020; Ic, *m/z* 1018 (Weijers et al., 2007b). Peak areas were integrated following the methods described in Weijers et al. (2007b). Each sample was measured at least three times or more, and measured over multiple days, to determine the analytical error associated with the precision and reproducibility of these analyses. The standard deviation was calculated for each sample and is plotted in figures with the 2σ (95%) confidence interval of the results.

Results and discussion

Age model for core LM2 from Lake McKenzie

The obtained ^{14}C AMS and ^{210}Pb dates from cores LM1 and LM2 are shown in Tables 1 and 2. A common depth axis for the adjacent cores was constructed using linear interpolation between tie-points identified on the %TOC curves (Fig. 2). A deposition model was constructed using the OxCal (v4.1) P_Sequence model ($k = 4$) (Bronk Ramsey, 2009). Three of the AMS ^{14}C dates were identified as being outliers (OZ0411, OZN680 and OZN681), and were excluded from deposition model calculations. The exclusion of these dates as outliers was based on: their poor fit with other radiocarbon dates based on linear regression, the lower overall Agreement Index produced when suspected outlying dates were included individually in P_Sequence deposition models, and the results of OxCal outlier analyses showing the dates as having higher posterior probabilities of being outliers compared with the other dates. The reason for these ^{14}C AMS dates yielding younger ages compared to the other samples is not currently known. Potentially the ^{14}C dates from pollen extracts may be affected by terrestrial reworking, which could result in these samples having older ^{14}C ages than the material produced within Lake McKenzie. Unfortunately, organic matter from core LM2 was not ^{14}C dated which potentially could have shed light on the potential reworking of terrestrial pollen. A large observed difference in the age of pollen from 26 to 27 cm depths indicates that almost no sedimentation occurred between ~14.0 ± 0.7 and 18.3 ± 0.5 cal ka BP (Fig. 3A) and therefore could represent a hiatus in sedimentation when Lake McKenzie may have dried or was ephemeral.

According to the ^{210}Pb and ^{14}C age models Lake McKenzie has experienced a wide range of sedimentation rates in the past: ~160 yr/cm at the bottom,~900 y/cm in the LGM section of the core, ~660 yr/cm after the hiatus in sedimentation and ~18 yr/cm in ^{210}Pb dated top section of core LM2. The low sedimentation rates in the ^{14}C dated sections of LM2 are in the range of other lakes on Fraser Island like Lake Coomboo Depression (~1000 y/cm, Longmore and Heijnis, 1999) and Lake Allom (~133 yr/cm, Donders et al., 2006). These low sedimentation rates are not unexpected as Fraser Island is a sand island dominated by rainforest vegetation, where sediment sources are few (Donders et al., 2006). Overall, Lake Allom exhibits higher sedimentation rates than Lake McKenzie which can be explained through differences in physical and chemical characteristics: Lake McKenzie has markedly clearer water, lower Total Phosphorus, Total Nitrogen and Ch-a content compared to Lake Allom (Bowling, 1988; Longmore, 1997; Hadwen, 2002). Whether these parameters are related to a low rate of productivity or high rate of sediment diagenesis, and thus a slow sediment accumulation rate at Lake McKenzie, remains to be tested.

The sediment accumulation rate calculated from $^{210}Pb_{unsupported}$ activity is much higher than that estimated for the underlying sediments dated using radiocarbon. The high water content, and low bulk density (Hembrow et al., 2014), of the upper layers of sediment may account in part for this shift in sediment accumulation rate at 7 cm depth. Higher densities and lower water content were observed ^{14}C dated sections of core LM2 densities observed in the 30–24 cal ka BP period (Hembrow et al., 2014) suggesting that sediment compaction is a factor in LM2. Additionally there may have been a reservoir age affecting the ^{14}C dates, which were based on pollen extracts, or a difference in the transport rates of the two types of material dated (fine grained organic material compared to ^{210}Pb carrying particles). Bioturbation does not appear to have played a major role at core LM2 in recent years as a clear monotonic decrease in $^{210}Pb_{unsupported}$ with depth is observed in the upper part of the record.

https://doi.org/10.1016/j.yqres.2014.02.005 Published online by Cambridge University Press

Table 1
Table of ^{14}C dates obtained from cores LM1 and LM2 from Lake McKenzie. LM1 depths have been converted to the core LM2 depth axis, based on linear interpolation between tie-points based on organic carbon percentages in both sediment cores.

Lab code	Loss corrected depth (cm)	Core	Composition	^{14}C ka BP	Error (1σ)	Calibrated age-range (cal yr BP; 2σ)
OZN683	11.9	LM2	Pollen	2395	±35	2183–2654
OZN684	17.1	LM2	Pollen	3785	±35	3931–4230
OZN685	22.1	LM2	Pollen	6485	±50	7260–7431
OZO411	24.8	LM2	Pollen	4,15	±40	5,09–5044
OZN686	26.6	LM2	Pollen	12,110	±70	13,786–14,148
OZO412	27.5	LM2	Pollen	15,100	±70	18,589–18,026
OZN687	31.2	LM2	Pollen	18,670	±100	21,872–22,545
OZN680	34.4	LM1	Pollen	19,150	±210	22,330–23,428
OZN681	34.4	LM1	Wood	13,188	±60	13,188–13,457
OZN688	36.3	LM2	Pollen	23,270	±120	27,785–28,499
OZN689	41.5	LM2	Pollen	30,940	±190	34,924–36,280
OZN690	47.2	LM2	Pollen	31,870	±180	35,575–36,783

With the current information however it is imposable to further evaluate the robustness of the age model for core LM2. However the timing of the LGM and a mid-Holocene temperature optimum in core LM2 (discussed below) agrees with marine record and therefore may be an indication that the age model for LM2 is not seriously biased.

Branched GDGT distributions as a potential palaeotemperature proxy for core LM2 and a strong observed agreement with the instrumental record

GDGT distributions in core LM2 were dominated by branched GDGT lipids, with isoprenoid GDGT lipids making up less than 5%. Branched GDGT distributions were dominated by branched GDGT 1 (*m/z* 1022), that contributed ~75% of all branched GDGT lipids.

A range of different soil (Weijers et al., 2007b; Peterse et al., 2012) and lake (Tierney et al., 2010; Zink et al., 2010; Pearson et al., 2011; Sun et al., 2011; Loomis et al., 2012) branched GDGT calibrations have been published that could be used to calculate temperatures. Loomis et al. (2012) use different branched GDGT ratios to calculate temperatures based on 1: the MBT/CBT ratio, 2: the main Branched GDGTs (MBR) or 3: a selection of branched GDGTs based on selective forward selection (SFS). Sun et al. (2011) calibrated both against MAAT or the temperature of the warm season (Tw). All calibrations were evaluated to determine whether the choice of calibration significantly affected the resulting paleotemperature reconstruction for Lake McKenzie (Fig. 4).

The selection of calibration was observed to have a significant effect on the resulting paleotemperature reconstructions (Fig. 4), although all calibrations indicated that MAAT was significantly lower during the end of the last glacial period compared to the Holocene. Among the different applied calibrations large disagreements were observed among the pattern and amplitude of past reconstructed temperature changes, as well as in the absolute values of the inferred temperatures (Fig. 4). The MAAT reconstruction using the soil calibrations (Weijers et al., 2007b; Peterse et al., 2012) and the MAAT and Tw calibrations of Sun et al. (2011) showed good agreement in the pattern of reconstructed MAAT, but differed in estimates of amplitude of past MAAT changes and the absolute values of inferred temperatures (Fig. 4). Similarly the Loomis et al. (2012) MBR and Zink et al. (2010) MBT reconstructions agreed in the trend of reconstructed MAAT, but differed in amplitude of MAAY changes and the values of inferred MAAT (Fig. 4). All other calibrations (Tierney et al., 2010; Pearson et al., 2011; Loomis et al., 2012 SFS and MBT) resulted in unique patterns of reconstructed MAAT variability within core LM2 (Fig. 4). The choice of calibration does affect the produced record of inferred temperatures from core LM2. Therefore it was important to determine which calibration provided the most accurate estimates of past temperature.

According to the ^{210}Pb age model, the top 1 cm slice of sediment from core LM2 covers a period of sediment accumulation between 1991 and 2005. Inferred MAAT values from this sediment based on the different calibration ranged from 18.1 to 40.7°C (Fig. 4, Table 3). Comparison of these estimates with an instrumental record may provide information about the performance of the different calibrations. The weather station located on the mainland at Maryborough (Fig. 1, of BOM weather station: 040126) is the nearest weather station that contained a complete record between 1991 and 2005. In overlapping years this weather station was in agreement with a nearer, but incomplete record of MAAT from Eurong (BOM weather station: 0040478) located near Lake McKenzie. Therefore absolute MAAT measured at Maryborough was assumed to be similar to that experienced at Lake McKenzie. Most calibrations yielded estimates of MAAT for the top 1 cm of sediment that were significantly higher than the instrumentally measured MAAT at Maryborough (21.5°C). The Pearson et al. (2011) or the Sun et al. (2011 Tw) calibrations were calibrated using warm season/summer temperatures and thus cannot be compared to instrumentally measured MAAT. Both soil calibrations of Weijers et al. (2007b) and Peterse et al. (2012) yielded MAAT estimates (25.4 and 20.4°C) that were, considering calibration errors (4.8 and 5.0°C), in agreement with instrumentally measured MAAT. None of the lake MAAT calibrations produced MAAT values that were near the instrumentally measured MAAT and with exception of the Tierney et al. (2010) calibration, all significantly overestimated inferred MAAT. With the limited information about the branched GDGT producers it would be speculative to assume that branched GDGTs in core LM2 would reflect a MAAT and not a seasonal temperature. Therefore the above observations are not sufficient to determine that soil calibrations were most applicable for inferring MAAT from core LM2.

Instead, the performance of each calibration was evaluated according to how accurately the trend and amplitude of past MAAT variability was reconstructed relative to a local instrumental temperature record. The top five sediment slices from core LM2 cover 95 yr of sediment accumulation (1910–2005), according to the ^{210}Pb age model. This therefore overlaps with local instrumental MAAT records. The above discussed weather station at Maryborough was not used for this comparison, as this long term temperature record was classified as potentially being affected by increased urban development in the late 20th century (BOM, 2013). Instead the MAAT record from Sandy Cape Lighthouse (BOM weather station: 039085) was used for evaluating the performance of the different calibrations. This weather station is located within a preservation area on Fraser Island, approximately 60 km north of Lake McKenzie (Fig. 1). At this weather station MAAT increased by approximately 1.0°C between 1910 and 2005 and both the amplitude and pattern of change were nearly identical to those observed in other regional and state-wide climate temperature records (BOM, 2013). For overlapping years the Sandy Cape Lighthouse recorded approximately 1.2°C higher temperatures compared to the weather stations at Eurong and Maryborough. This higher temperature may be in part explained by the

https://doi.org/10.1016/j.yqres.2014.02.005 Published online by Cambridge University Press

Table 2
Total ^{210}Pb, Supported ^{210}Pb, Unsupported ^{210}Pb, and particle size results for samples taken from core LM1. Calendar age estimates using the CIC and CRS models are shown (Appleby and Oldfield, 1978; Appleby, 2001). Both the original depths measured on core LM1 and the corresponding depths on core LM2 are shown.

ANSTO ID	Depth Interval measured on core LM1 (cm)	Corresponding depth interval on core LM2 (cm)	Total ^{210}Pb (Bq/kg)	Supported ^{210}Pb (Bq/kg)	Unsupported ^{210}Pb[a] (Bq/kg)	Particle size ≤62.5 μm (%)	Calculated CIC age (years)	Calculated CRS age (years)
M897	0.00–0.25	0.0–0.7	614.4 ± 12	14.1 ± 2	601.2 ± 12	74.0	5 ± 5	5 ± 2
M898	0.25–0.50	0.7–1.4	490.8 ± 24	17.5 ± 2	483.7 ± 24	74.0	15 ± 5	13 ± 4
M899	1.50–1.75	4.1–4.8	168.3 ± 6	18.7 ± 2	149.9 ± 6	90.0	65 ± 7	64 ± 8
M900	1.75–2.00	4.8–5.5	97.9 ± 4	14.7 ± 2	85.0 ± 5	77.6	75 ± 8	76 ± 9
M901	3.00–3.50	7.0–7.8	31.0 ± 1	19.6 ± 2	11.5 ± 2	83.9	131 ± 14	130 ± 11
M902	4.50–4.75	9.4–9.8	37.6 ± 1	27.0 ± 3	10.6 ± 3	78.9	–	–
M903	4.75–5.00	9.8–10.2	75.6 ± 4	63.1 ± 6	12.8 ± 7	79.9	–	–
N369	6.00–6.25	11.7–12.2	85.9 ± 4	21.9 ± 3	66.7 ± 5	69.9	–	–
N370	6.25–6.50	12.2–12.6	101.8 ± 5	42.3 ± 4	61.8 ± 6	72.5	–	–
N371	7.00–7.25	13.4–13.8	33.8 ± 2	32.9 ± 3	0.9 ± 4	73.3	–	–
N372	7.25–7.50	13.8–14.2	30.9 ± 2	32.9 ± 3	Not detected	83.5	–	–
N373	8.00–8.25	15.0–15.2	62.6 ± 3	28.2 ± 3	35.8 ± 4	81.5	–	–
N374	8.25–8.50	15.2–15.5	62.5 ± 3	32.2 ± 3	31.5 ± 5	68.7	–	–

[a] Decay corrected to a fixed date.

lower latitude of the Sandy Cape Lighthouse compared to Eurong and Lake McKenzie. Additionally the location of Sandy Cape Lighthouse may reflect more marine like climate compared to Eurong and Maryborough which may explain the average higher temperature at this station. Besides this systematic offset in MAAT, both the pattern and amplitude of changes in MAAT observed between 1910 and 2005 are assumed to have been similar at both Sandy Cape Lighthouse and Lake McKenzie.

All of the branched GDGT calibrations produced temperature reconstructions that were significantly correlated ($P < 0.05$) with the instrumental record of average MAAT. The observed correlation coefficients of these comparisons ranged between 0.618 and 0.961 and the six most strongly correlated ($R^2 = 0.929$–0.961) cross-plots are shown in Figure 5. Of the six most strongly correlated calibrations, five used CBT/MBT ratios to infer temperature from branched GDGT distributions. These high correlation coefficients suggest that those calibrations accurately captured the trend of MAAT changes. Besides reconstructing the trend, the best calibration should also be able to quantitatively reconstruct the amplitude of MAAT changes. This can be evaluated by comparing the slope value of the relationship between instrumental and reconstructed MAAT, where the most accurate calibration would have a value near 1. The soil calibration of Peterse et al. (2012) produced a value for the slope that was very close to one, while all other highly correlated calibrations produced slope values that were significantly higher than one (Fig. 5). These higher slope values indicate that these calibrations may substantially overestimate the reconstructed amplitude of MAAT changes. The soil calibration of Peterse et al. (2012) accurately captured both the trend and amplitude of observed MAAT changes during the studied period and therefore seems the calibration of choice for quantitatively inferring temperatures from core LM2. To our knowledge, this is the first time such good agreement has been observed between an instrumental temperature record and branched GDGT temperature reconstruction from a lacustrine sediment core providing confidence in the qualitative quality of the produced MAAT record.

This good agreement between branched GDGT inferred and instrumental temperatures in LM2 may be seen as remarkable considering the large calibration error of the Peterse et al. (2012) calibration and the observed analytical error (≤0.4°C). However, when comparing temperature estimates from a single sediment core the overall uncertainty caused by the calibration error may be significantly less than 5°C. The large scatter of the Peterse et al. (2012) calibration is likely reflecting that besides pH and temperature, other environmental, geological or biological factors may affect branched GDGT distributions in the global soil data set, and these are not being accounted for. It is likely that these unincorporated factors vary to a much greater degree within a global data set compared to a single location or sediment record (Peterse et al., 2011). The actual influence of the calibration error on the reconstructed trend and amplitude of the MAAT reconstruction from this single sediment core may be considered to be relatively small or systematic in nature. Although a local calibration would be required to determine the actual uncertainty in the inferred temperature estimates from core LM2, the nearly identical pattern of inferred and instrumentally measured MAAT does not suggest that the large calibration error of the Peterse et al. (2012) calibration had a significant effect on the accuracy of the reconstructed pattern and amplitude of MAAT changes. Additionally, the good agreement between instrumental and inferred MAAT in LM2 shows that by measuring each sample at least in triplicate, and comparing mean temperature estimates, relatively small temperature changes (<1°C) appear to be accurately reconstructed.

An allochthonous origin of branched GDGTs in the sediment of Lake McKenzie

That the calibration of Peterse et al. (2012) accurately reconstructed both the trend and amplitude of past MAAT variability, suggests an allochthonous and probably a soil derived origin of the branched GDGTs observed in the Lake McKenzie sediments. A comparison between the environmental parameters and branched GDGT distributions observed in soils and the lake sediment could provide evidence for this.

There is a significant difference in the pH of the water column of Lake McKenzie and the soils surrounding the lake: the soils surrounding Lake McKenzie consist of rapidly draining aeric podosols that are only slightly acidic (pH = 5.8, McKenzie et al., 2004), whereas the water column of Lake McKenzie is acidic over the entire annual cycle (pH 3.7–4.8, Hadwen, 2002). This difference in pH combined with the sensitivity of branched GDGT distributions to pH, provides an opportunity to compare branched GDGT distributions measured in soils and the lake sediment to determine whether the branched GDGTs observed in the sediment of Lake Mckenzie are of predominantly allochthonous or autochthonous origin.

The branched GDGT distributions determined in three soil samples (top 10 cm) surrounding Lake McKenzie were observed to be nearly identical to those observed in the top 1 cm sediment slice of core LM2 in Lake McKenzie (Fig. 6A). In both the soils and in the top sediment slice, branched GDGT distributions are dominated by branched GDGT 1 (*m/z* 1022) which is a feature more commonly observed in soil samples, rather than lake sediments that may contain branched GDGTs produced in situ (Fig. 6B). These observations are consistent with a predominantly allochthonous origin for the branched GDGTs observed in Lake McKenzie.

https://doi.org/10.1016/j.yqres.2014.02.005 Published online by Cambridge University Press

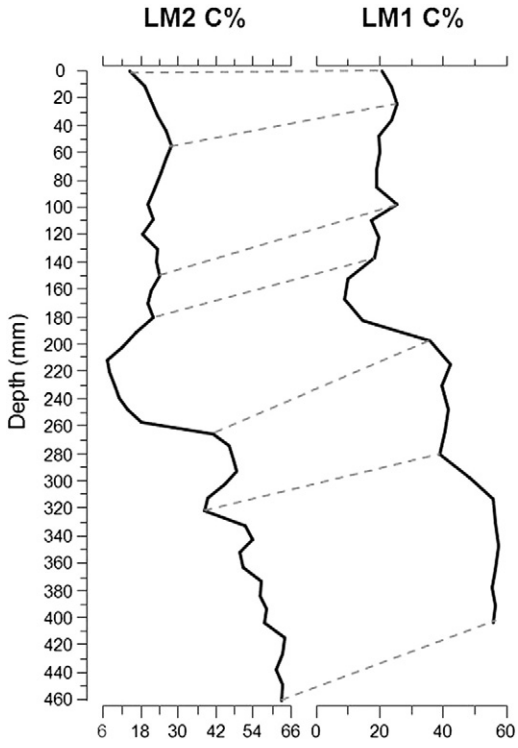

Figure 2. Tie-points between adjacent cores LM1 and LM2 based on organic carbon percentages. Depths from dated intervals from the LM1 core were transferred to core LM2 based on the assumption of linear sedimentation between these tie points.

Further potential evidence of a predominantly allochthonous origin of branched GDGTs in Lake McKenzie was observed from the CBT reconstructed pH values from both the sediment slice and the soil samples (Fig. 7). Depending on which CBT calibration was applied, pH estimates from the top sediment slice ranged from 5.9 (Peterse et al., 2012), to 6.1 (Weijers et al., 2007b) and to 7.1 (Sun et al., 2011). These pH estimates were all significantly higher (higher than the calibration errors of the pH estimates based on branched GDGTs) than the pH of the water column of Lake McKenzie. Instead the reconstructed pH value of Lake McKenzie sediment was nearly identical to both the pH estimate and published pH for the soils surrounding Lake McKenzie (Fig. 7). This and the information discussed above, suggests that in situ production of branched GDGTs in Lake McKenzie is either minor or non-existent, and this supports the application of the Peterse et al. (2012) soil calibration to infer temperatures and pH values from the branched GDGTs observed in core LM2 from Lake McKenzie.

Independence of the LM2 temperature reconstruction

There appears to be some degree of synergy among the reconstructed MAAT, pH and %TOC values determined in core LM2 (Fig. 8A). Both inferred MAAT and pH estimates from LM2 indicated higher temperatures and pH values in the Holocene section compared to the end of the Last Glacial section of the record. In contrast, % TOC of the sediments was observed to be significantly lower in the Holocene and high during the end of the Last Glacial sections of the record from LM2. Tyler et al. (2010) previously observed a strong correlation between the CBT and MBT ratios in Lochnagar suggesting that in this lake apparent changes in reconstructed temperatures were controlled by changing pH values. No correlation between the CBT and MBT ratios was observed in the LM2 record (Fig. 8B). Both pH and temperature were reconstructed to be low during the end of the Last Glacial and higher during the Holocene periods and there appears to be a significant degree of correlation ($R^2 = 0.872$) between these parameters when the entire record is compared. However the strength of this correlation is reduced to insignificant values (0.373 and 0.183) when pH and MAAT are compared separately for the end of the Last Glacial and Holocene periods (Fig. 8C). The observed independence of the MBT from the CBT ratio and the lack of correlation between trends of temperatures and pH during the end of the Last Glacial and the Holocene periods suggest that the reconstructed trend of MAAT variability was not controlled by changes in pH. Similarly, the relationship between % TOC and reconstructed MAAT appeared to be significantly inversely correlated ($R^2 = 0.658$) when values from the entire record were assessed, but the correlation is observed to be either insignificant ($R^2 = 0.258$) at the end of the Last Glacial or significant ($R^2 = 0.673$) during the Holocene, but in an opposite direction to the relationship observed over the entire record (Fig. 8D). Based on the limited information obtained in this study, no clear evidence indicated that the apparent MAAT reconstruction from Lake McKenzie was controlled by any environmental parameters other than temperature, and therefore the MAAT reconstruction was interpreted as reflecting an independent MAAT record.

Trend and amplitude of MAAT changes as reconstructed from core LM2

Due to low sedimentation rates, the 46 cm long LM2 sediment core provided information about trend of MAAT variability at subtropical eastern Australia going as far back as 37 cal ka BP. The resolution of the LM2 MAAT record is relatively low due to the slow sedimentation rates and the 1 cm thick sample slices. Still, the LM2 record provides information about at least millennium scale MAAT variability at coastal subtropical eastern Australia during Marine Oxygen Isotope Stage 3 (MIS 3), the Last Glacial, and the Holocene periods. An apparent hiatus in sedimentation between 18.3 and 14.0 cal ka BP resulted in the LM2 record not providing information about the trend of MAAT during a large portion of the Last Glacial termination. As discussed above, the good agreement with the instrumental and LM2 record indicates that the LM2 MAAT reconstruction potentially provides quantitative estimates of the amplitude of MAAT variability. However, a lack of other quantitative temperature reconstructions from coastal subtropical eastern Australia made it impossible to validate the apparent quantitative nature of the reconstructed trend and amplitude of MAAT variability at Lake McKenzie prior to 1910, when standardized temperature measurements began at weather stations in Australia (BOM, 2013). Instead the produced Lake McKenzie MAAT record was compared to other climate records from within the Australian region and discussed in a paleoclimate perspective for the different climate periods.

37–30 ka, Late MIS 3

Between 37.3 ± 0.4 and 31.6 ± 0.7 cal ka BP, reconstructed temperatures in the LM2 record were relatively stable and substantially warmer than between 30.2 ± 0.6 and 18.8 ± 0.5 cal ka BP (Fig. 9). All MAAT estimates between 37 and 32 ka were observed to be statistically similar and therefore did not suggest significant millennium scale temperature variability. Ice core records from Antarctica do show millennium scale temperature variability through this period with temperature changes up to 2°C (EPICA, 2006). Perturbations in temperature were also observed in the Murray Canyons, offshore from Southern Australia (De Deckker et al., 2012) and in deep oceanic cores from the Southern ocean (Barrows et al., 2007; Armand and Leventer, 2010). A lack of perturbations in the LM2 MAAT record suggests that subtropical eastern Australia did not experience a similar change in temperature through this period, although the resolution was not high through this period. This would be in agreement with other low latitude continental records from the southern hemisphere (Tierney et al., 2008; Woltering et al., 2011).

https://doi.org/10.1016/j.yqres.2014.02.005 Published online by Cambridge University Press

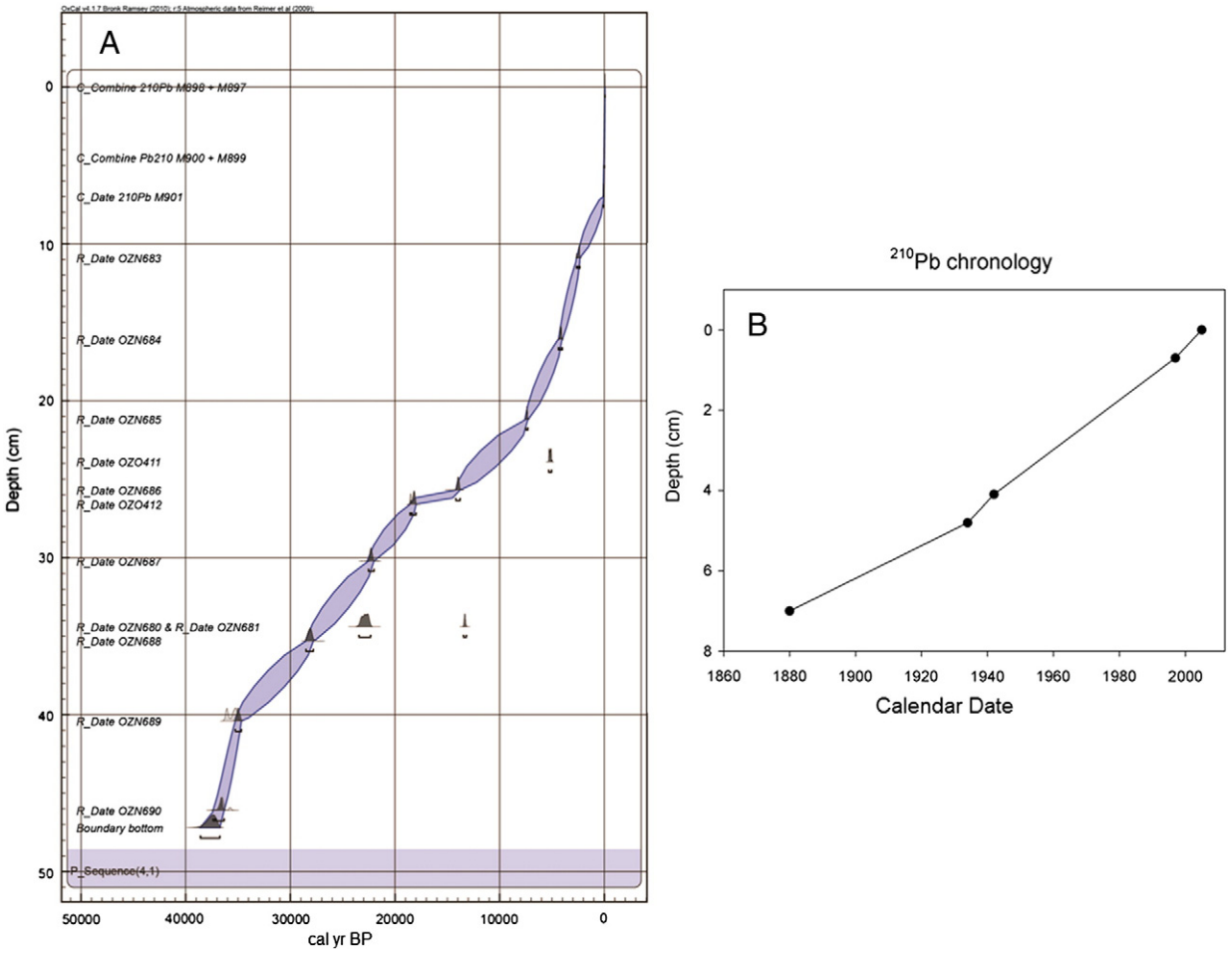

Figure 3. A: Age model for core LM2 constructed using the P_sequence deposition program in OxCal 4.1 and the IntCal 09 calibration curve (Bronk Ramsey, 2009; Reimer et al., 2009). Three ^{14}C dates were tagged as outliers (OZ0411, OZN680 and OZN681). ^{210}Pb dates with very small depth differences were combined. Combined pairs were dates M898 and M897, and M900 and M899. B: A separate age model was developed for the uppermost section for core LM2 based on the transferred ^{210}Pb dates from core LM1 using linear interpolation between tie-points based on the organic carbon percentage curves. Age estimates for the upper 7 cm of the core were determined using linear interpolation, and an extrapolation based on the ^{210}Pb dated horizons.

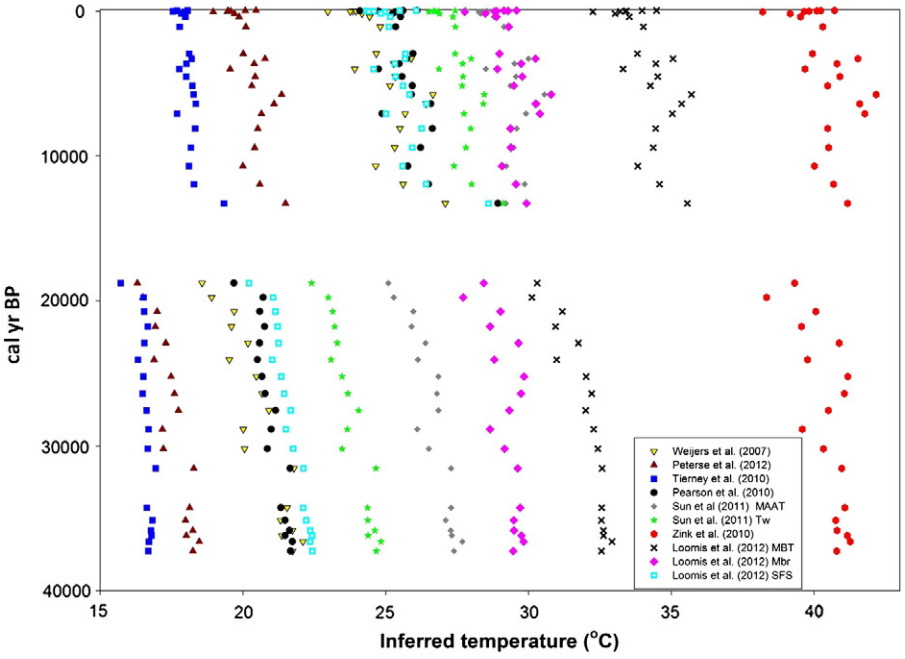

Figure 4. Reconstructed temperatures based on different branched GDGT calibrations. The selection of calibration is shown here to have a significant effect on both absolute reconstructed temperature and the amplitude of past temperature variability. *ages were interpolated from the age model, where zero means AD 1950.

https://doi.org/10.1016/j.yqres.2014.02.005 Published online by Cambridge University Press

Table 3
Depths (not corrected for loss due to compaction), ages and inferred temperatures using different branched GDGT calibrations as measured in core LM2 from Lake McKenzie. MAAT = Mean Annual Air Temperature, MSAT = Mean Summer Air Temperature. *ages were interpolated from the age model where zero mean AD 1950.

Uncorrected	Average age		MAAT (°C)		MAAT (°C)		MAAT(°C)		Tw (°C)		MAAT (°C)		MAAT (°C)	
Depth in core (cm)	(cal yr BP)	±	Weijers et al.(2007b)	±	Peterse et al. (2012)	±	Sun et al. (2011)	±	Sun et al. (2011)	±	Loomis et al. (2012)SFS	±	Loomis et al. (2012) MBR	±
0.5	−48	7	25.4	0.7	20.5	0.4	29.6	0.5	27.8	0.4	26.1	0.8	29.6	0.6
1.5	−32	9	24.8	0.2	20.1	0.2	29.1	0.2	27.4	0.2	25.5	0.6	29.1	0.3
2.5	−14	9	23.9	0.2	19.5	0.1	28.5	0.1	26.7	0.1	24.3	0.3	29.3	0.1
3.5	3	8	24.0	0.6	19.6	0.4	28.6	0.4	26.9	0.4	24.6	0.6	28.9	0.2
4.5	22	11	23.8	0.5	19.5	0.3	28.4	0.4	26.7	0.3	24.4	0.3	28.8	0.5
5.5	43	10	23.0	0.6	19.0	0.4	28.3	1.2	26.5	0.3	25.0	0.2	27.8	0.5
6.5	174	121	24.2	1.0	19.7	0.6	28.3	0.3	26.9	0.1	24.8	0.3	28.5	0.5
7.5	393	99	24.4	0.3	19.9	0.2	28.8	0.2	27.4	0.2	25.2	0.3	28.9	0.3
8.5	1083	591	24.8	0.3	20.1	0.2	29.2	0.2	27.4	0.3	25.1	0.5	29.3	0.1
11.5	2939	163	24.7	0.7	20.0	0.4	29.0	0.5	27.4	0.4	25.7	0.4	29.0	0.6
12.5	3284	182	25.9	0.2	20.8	0.1	30.0	0.1	28.0	0.4	25.7	1.2	30.2	0.7
13.5	3631	164	25.3	0.4	20.4	0.3	29.5	0.3	27.7	0.2	25.3	0.4	29.7	0.2
14.5	3996	201	23.9	0.5	19.6	0.3	28.5	0.4	26.9	0.2	24.6	0.3	28.9	0.5
15.5	4523	326	25.3	0.5	20.4	0.3	29.6	0.4	27.7	0.2	25.3	0.3	29.8	0.6
16.5	5153	304	25.2	0.3	20.3	0.2	29.4	0.2	27.7	0.2	25.6	0.1	29.5	0.3
17.5	5761	304	26.7	0.4	21.4	0.2	30.6	0.4	28.5	0.2	25.8	0.2	30.8	0.4
18.5	6399	334	26.4	0.3	21.1	0.2	30.3	0.3	28.4	0.1	26.4	0.3	30.3	0.5
19.5	7083	351	25.7	0.5	20.7	0.3	29.9	0.4	27.7	0.2	25.0	0.3	30.4	0.5
20.5	8108	674	25.5	0.3	20.5	0.2	29.6	0.3	28.0	0.1	26.3	0.1	29.4	0.3
21.5	9424	642	25.3	0.7	20.4	0.5	29.5	0.6	27.8	0.4	25.9	0.4	29.4	0.5
22.5	10699	633	24.7	0.1	20.0	0.1	29.2	0.5	27.4	0.0	25.6	0.1	29.1	0.2
23.5	11949	618	25.6	0.3	20.6	0.2	29.9	0.4	28.0	0.2	26.4	0.2	29.6	0.2
24.5	13275	708	27.1	0.7	21.5	0.4	29.2	2.9	29.1	0.6	28.6	1.3	29.9	0.2
26.5	18784	500	18.6	0.7	16.3	0.4	25.1	0.4	22.4	0.7	20.2	0.8	28.4	0.4
27.5	19767	484	18.9	0.6	16.5	0.4	25.3	0.5	23.0	0.4	21.1	0.2	27.7	0.4
28.5	20740	489	19.7	0.6	17.0	0.4	26.0	0.5	23.1	0.3	21.1	0.1	29.0	0.7
29.5	21779	550	19.6	0.3	16.9	0.2	25.9	0.3	23.2	0.0	21.2	0.0	28.7	0.6
30.5	22913	584	20.2	0.7	17.3	0.4	26.4	0.4	23.3	0.5	21.2	0.2	29.6	0.3
31.5	24048	552	19.5	0.8	16.9	0.5	26.1	0.7	23.1	0.5	21.0	0.3	28.8	0.6
32.5	25215	616	20.5	0.1	17.5	0.1	26.9	0.3	23.5	0.0	21.3	0.0	29.8	0.3
33.5	26388	557	20.7	0.8	17.6	0.5	26.8	0.6	23.7	0.4	21.4	0.2	29.7	0.5
34.5	27550	605	20.9	0.5	17.7	0.3	26.9	0.5	24.1	0.2	21.7	0.1	29.3	0.9
35.5	28852	697	20.0	0.5	17.2	0.3	26.1	0.3	23.7	0.3	21.5	0.2	28.7	0.4
36.5	30198	649	20.1	0.2	17.2	0.1	26.5	0.5	23.5	0.2	21.8	0.3	29.2	0.4
37.5	31556	710	21.8	0.5	18.3	0.3	27.3	0.4	24.7	0.4	22.1	0.2	29.6	0.3
39.5	34267	700	21.6	0.7	18.1	0.4	27.3	0.4	24.4	0.4	22.1	0.2	29.7	0.4
40.5	35138	171	21.3	0.5	18.0	0.3	27.1	0.3	24.4	0.3	22.2	0.2	29.5	0.3
42.5	35843	169	21.7	0.4	18.3	0.3	27.3	0.4	24.6	0.3	22.4	0.2	29.5	0.3
43.5	36193	180	21.4	0.4	18.0	0.2	27.3	0.4	24.4	0.3	22.4	0.3	29.8	0.5
44.5	36613	240	22.1	0.3	18.5	0.3	27.7	0.4	24.8	0.3	22.4	0.5	29.8	0.7
45.5	37261	407	21.7	0.4	18.3	0.2	27.4	0.3	24.7	0.3	22.4	0.3	29.5	0.1

30–22 ka, early last glacial period

Between ~30.2 ± 0.6 and 28.9 ± 0.7 cal ka BP, temperatures in the LM2 record dropped by ~1°C relative to the period between 37.3 ± 0.4 and 31.6 ± 0.7 cal ka BP (Fig. 9). The timing of this agrees with studies from Antarctica (Blunier and Brook, 2001), Chile (Denton et al., 1999) and New Zealand (Hellstrom et al., 1998; Vandergoes et al., 2005), that all document cooling at ~30 ka, potentially as a result of an insolation minimum in the Southern Hemisphere (Vandergoes et al., 2005). However *Globigerinoides ruber* ^{18}O record from core GC-12 located approximately 220 km north of Lake McKenzie, did not show a similar decrease of temperature around 30 cal ka BP (Bostock et al., 2006, Fig. 10). This difference between proximate temperature records may be due to the LM2 reconstruction being land derived, and therefore more sensitive to changes in radiative forcing relative to the ocean. MAAT increased by approximately 0.5°C compared to 30.2 ± 0.6 and 28.9 ± 0.7 cal ka BP, after which the trend in MAAT values showed a general decline in temperatures towards the LGM (Fig. 9). This cooling trend appeared to have started at approximately 27 cal ka BP in the LM2 record. This general trend can be also seen in GC-12 marine $\delta^{18}O$ record (Bostock et al., 2006, Fig. 10). A short period of warming and drying in the early glacial period between 26 and 24 ka was seen in paleoclimate reconstructions from the Australian region (Calvo et al., 2007; Moss and Kershaw, 2007; Armand and Leventer, 2010; Bowler et al., 2012). This coincided with the Kawakawa tephra and the first interstadial of the Last Glacial period in New Zealand (Barrell et al., 2013). A warming period was not observed in the LM2 record during this time period, although this short temperature anomaly could be missed due to poor chronological control and resolution combined with the uncertainty of the MAAT estimates. At Lake Allom and Old Lake Coombo depression, on Fraser Island to the north of Lake McKenzie, a hiatus in sedimentation was observed between 28 and 10 cal ka BP suggesting that during this entire period, conditions on Fraser Island were relatively dry (Donders et al., 2006).

22–18 ka, Last Glacial Maximum

The LGM globally is considered to have occurred between 27 and 19 ka (Clark et al., 2009). For Australia the timing of the LGM was defined to have started later; it centred on ~21 ka (Suggate, 1990) and lasted 3–4 ka (Bowler, 1976; Harrison, 1993; Barrows et al., 2001), or occurred from 23 to 18 cal ka BP (Kershaw, 1986; D'Costa et al., 1989; Turney et al., 2006) and was characterized by limited glacial advances in the Snowy Mountains and Tasmanian Highlands. Both of these regions recorded a maximum glacier extent at ~19 ka. The lowest temperature estimate observed in the

https://doi.org/10.1016/j.yqres.2014.02.005 Published online by Cambridge University Press

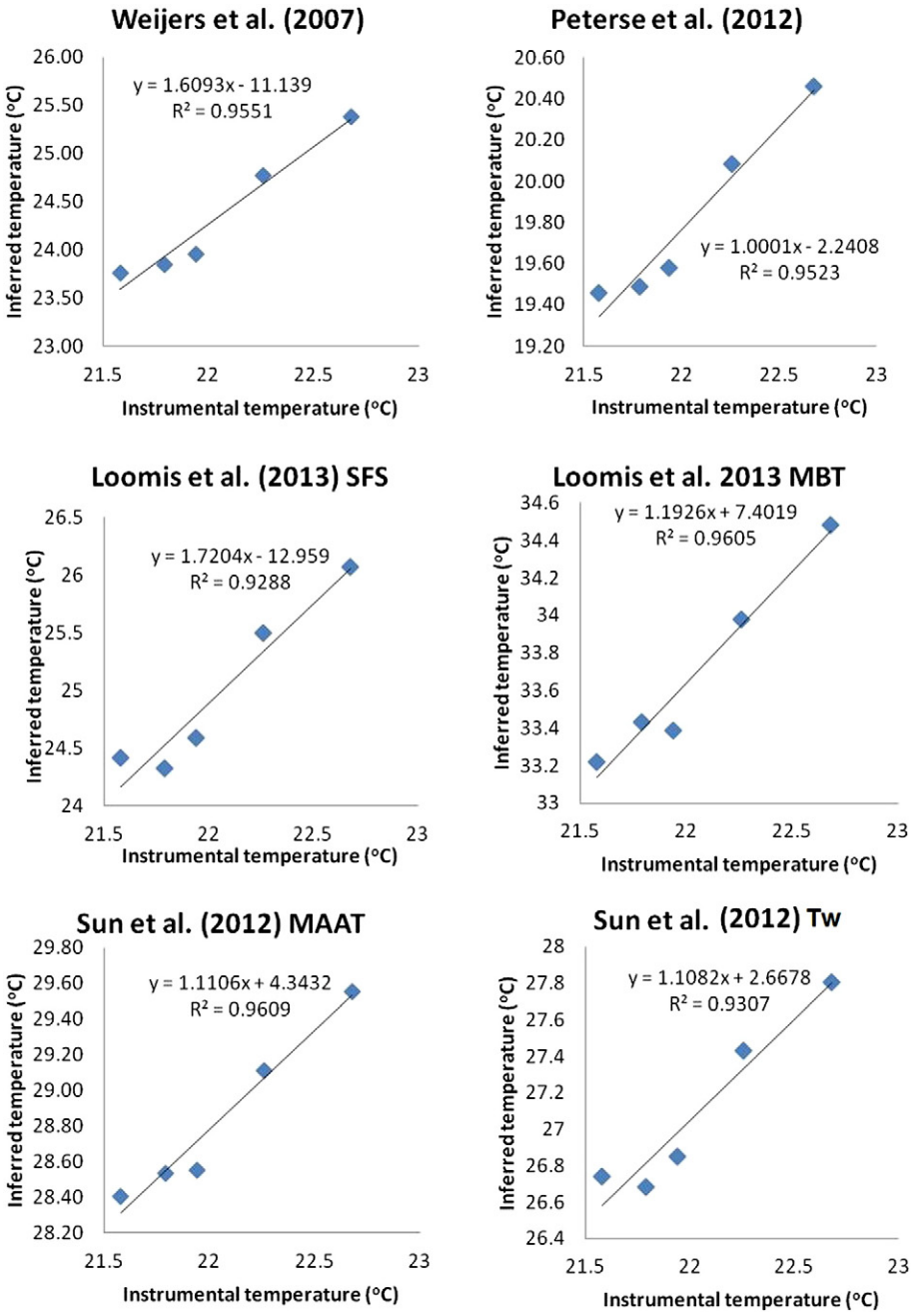

Figure 5. Graphs depicting the correlations between instrumentally measured mean air temperatures at Sandy Cape Lighthouse on Fraser Island and inferred temperatures using different soil and lacustrine calibrations for Lake McKenzie core LM2 branched GDGTs. Application of the soil calibration by Peterse et al. (2012) produces both a strong correlation between instrumental and inferred temperatures, and a regression line slope that is close to 1, suggesting that the calibration provides an accurate estimate of the amplitude of temperature variability.

LM2 MAAT occurs at 18.8 ± 0.5 cal ka BP, ~4.1°C lower than modern day temperature (Fig. 9). This was immediately followed by a hiatus in sedimentation between 18.3 and 14.0 cal ka BP. The timing of the lowest temperatures during the LGM ~19 cal ka BP in the Lake McKenzie record is in good agreement with $\delta^{18}O$ *G. ruber* records from the north (GC-12) and south (GC-25) of Fraser Island (Troedson and Davies, 2001; Bostock et al., 2006) (Fig. 10). This estimate of the maximum temperature anomaly of the LGM observed in core LM2 is slightly larger than a previously published foraminifera assembly study that estimates a 1–3°C anomaly for the subtropical west Pacific Ocean (Barrows and Juggins, 2005). $\delta^{18}O$ values in core GC-12 recorded 2–3°C lower temperatures, while GC-25 yielded $\delta^{18}O$ values that indicated temperatures were 6°C colder (Troedson and Davies, 2001). Bostock et al. (2006) interpreted this difference of temperature amplitude of the LGM between cores GC-12 and GC-25 to reflect a northwards shift in the separation of the Tasman Front from the EAC during the LGM, resulting in warm waters from the EAC not reaching GC-25. The ~4.1°C lower MAAT during the LGM observed in the LM2 reconstruction lies between the reconstructed amplitudes of cores GC-12 and GC-25 which may indicate that the separation of the EAC and the Tasman Front may have occurred more northerly than Lake McKenzie (25°26′S). Alternatively the intermediate LGM anomaly in the LM2 record may be explained by the effects of lowered sea level at the end of the LGM that resulted in an increased distance between Lake McKenzie and the west Pacific Ocean of approximately 60 km. This may have reduced the influence of the EAC on the climate of Lake McKenzie leading to more cooling at Lake

https://doi.org/10.1016/j.yqres.2014.02.005 Published online by Cambridge University Press

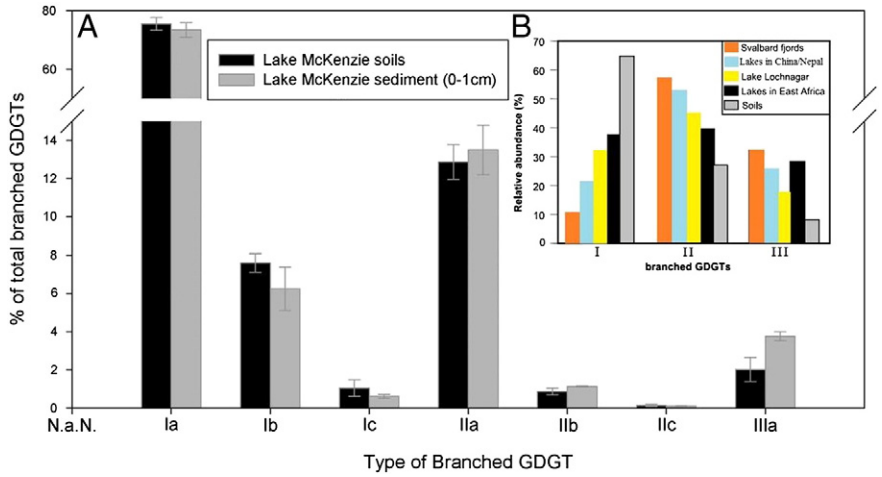

Figure 6. A: The relative distribution of branched GDGT lipids measured in 3 soil samples collected within the Lake McKenzie drainage basin and in the top sediment of core LM2. The largely identical branched GDGT signals suggest a predominantly soil origin of the branched GDGT in the sediments of Lake McKenzie. B: Average values of 3 prominent branched GDGTs in lake and fjord sediments affected by in situ production of branched GDGTs (Tierney et al., 2010; Tyler et al., 2010; Sun et al., 2011) and the average distribution in soils of the global soil calibration (Weijers et al., 2007b) (this figure is modified from Sun et al., 2011). The branched GDGT distribution in Lake McKenzie largely follows the typical global soil GDGT distribution, and is significantly different to sediments where there is evidence of in situ production of branch GDGTs.

McKenzie compared to sites more northerly in the subtropical west Pacific Ocean.

13.3–12.0 ka, end of last glacial termination period

Inferred temperatures are highest in the entire record just after the restart of sedimentation ~14 cal ka BP. (Fig. 9). The inferred temperature of ~21.5°C at 13.3 ± 0.7 cal ka BP was approximately 1.1°C higher than modern day MAAT. This may potentially indicate that relatively warm conditions occurred on Fraser Island during the Antarctic Cold Reversal or during the early Younger Dryas. A similar high temperature at this time was not observed in nearby $\delta^{18}O$ records from cores GC-12 (Bostock et al., 2006) and GC-25 (Troedson and Davies, 2001) (Fig. 10) or other records from the Australia region. Unless the temperatures at Fraser Island were totally decoupled from nearby locations, it seems unlikely that the peak in MAAT observed in the Lake McKenzie record at 13.3 ± 0.7 cal ka BP only occurred at this location. It is not possible to exclude the possibility that this high temperature may be the result of a change in source location or seasonality of branched GDGTs produced during and immediately following the hiatus period.

12–8 ka, early to mid Holocene

In the early Holocene between 12.0 ± 0.6 and 8.1 ± 0.7 cal ka BP, temperatures were observed to be near present day temperatures in the LM2 record (Fig. 9). This onset of modern day temperatures early in the Holocene is observed in other paleotemperature proxy records in the Southern Hemisphere (Shakun et al., 2012) and in the central Indo Pacific Warm Pool (IPWP) (Gagan et al., 2004). In comparison, SST in the tropical and temperate regions of Australia moved towards modern day temperatures between ~11 and 9 ka (Petherick et al., 2013; Reeves et al., 2013). Compared to the nearby marine ^{18}O temperature records GC-12 and GC-25, the LM2 reconstruction reached near modern day temperatures earlier than the surrounding oceans, which showed modern day conditions established at approximately 9 ka (Troedson and Davies, 2001; Bostock et al., 2006) (Fig. 10). An earlier onset of modern day temperatures of Fraser Island compared to surrounding oceans may be related to the higher sensitivity of terrestrial environments to changes in insolation compared to the delayed response of the oceans due to the higher heat content of the oceans relative to the atmosphere. The observations from the LM2 temperature record together with pollen evidence from Lake Allom on Fraser Island (Donders et al., 2006) suggest that the early Holocene was a period of relatively warm and dry conditions of Fraser Island.

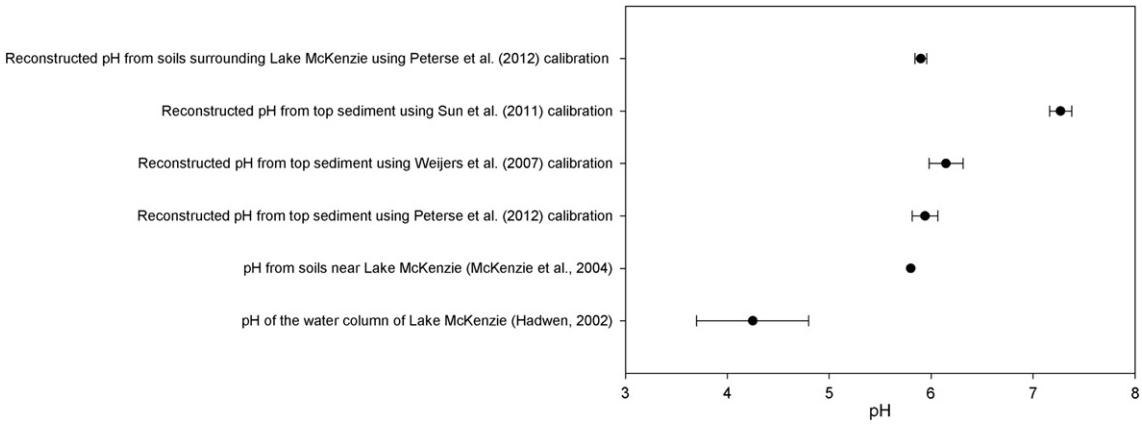

Figure 7. pH values obtained from the literature compared to reconstructed pH based on the soil and lake calibrations (Weijers et al., 2007b; Sun et al., 2011; Peterse et al., 2012). Reconstructed pH for the top 1 cm of core LM2 using the soil calibrations is consistent with previous measurements of soil pH in the region (McKenzie et al., 2004) and reconstructed pH values for soil samples surround the lake and is substantially higher than the measured pH of the lake water (Hadwen, 2002).

https://doi.org/10.1016/j.yqres.2014.02.005 Published online by Cambridge University Press

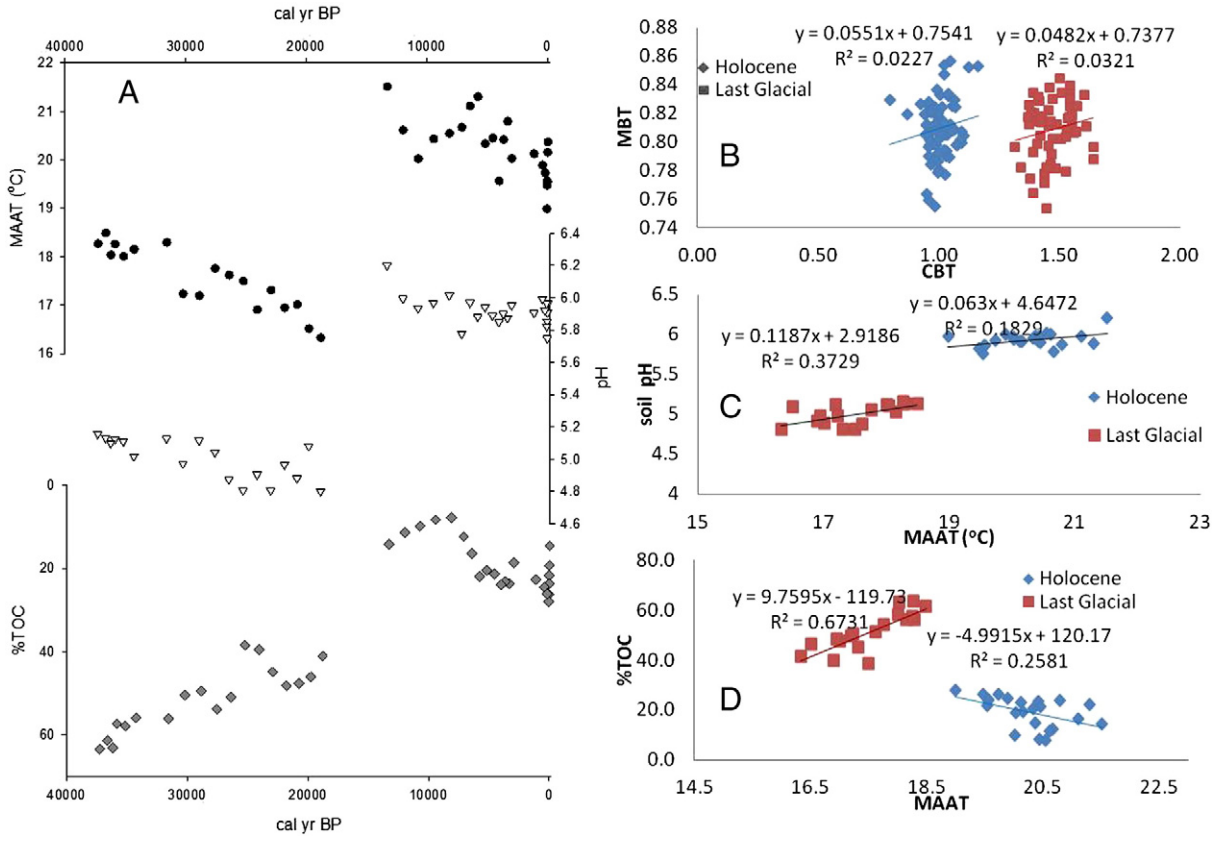

Figure 8. A: Branched GDGT inferred MAAT plotted together with inferred pH values and measured percentages of total organic carbon (%TOC) in core LM2 from Lake McKenzie, B: cross plot of CBT/MBT ratio, C: Cross plot of MAAT and pH and D: cross plot MAAT and %TOC.

8–5 ka, mid Holocene

The mid Holocene period in the Australasian region represents a period when maximum temperatures are observed in terrestrial records, although the highest temperatures appear to occur at slightly different times in different regions (Reeves et al., 2013). Antarctic temperatures stabilized during this period (EPICA, 2004) and in the North the thermal maximum of the IPWP occurred by 6.8–5.5 cal ka BP (Abram et al., 2009). During the mid-Holocene (7.1 ± 0.4 and 5.8 ± 0.3 cal ka BP) observed temperatures in the LM2 record were higher than the present (Fig. 9). The highest temperature was observed 5.8 ± 0.3 cal ka BP and was approximately 0.9°C higher than present day MAAT. This period corresponded with the timing of a thermal optimum of the IPWP (Abram et al., 2009), although chronological control of the LM2 record is low. The timing of this mid Holocene temperature maximum corresponded with a hiatus in the Lake Allom sediment record between 6.5 and 5.4 cal ka BP (Donders et al., 2006), suggesting that the period of elevated temperature detected at Lake McKenzie was likely a period of reduced effective precipitation on Fraser Island. Interestingly, the GC-12 and GC-25 $\delta^{18}O$ marine records from the north and south of Fraser Island did not exhibit a mid Holocene temperature optimum (Troedson and Davies, 2001; Bostock et al., 2006) (Fig. 10). An almost identical temperature anomaly of 1°C for the mid-Holocene temperature maximum as seen for LM2 has been previously reported for the central Great Barrier Reef, based on Sr/Ca ratios in corals from Orpheus Island (Gagan et al., 1998), although some questions about both the chronology of this coral record (Gagan et al., 1998) and the LM2 record remain.

5–0 ka, late Holocene

After the mid-Holocene, temperatures were lower, with values that were near or below present day MAAT between 5.2 ± 0.3 and 2.9 ± 0.2 cal ka BP. Directly after the mid Holocene thermal optimum, MAAT showed a large fluctuation where the MAAT dropped by 1.8°C over a period of approximately 1.8 ka followed by a warming of ~1.2°C over 0.7 ka (Fig. 9). At around the same time a high-resolution deep sea $\delta^{18}O$ record of *Globigerina bulloides* from South Australia showed several ~1500 yr cycles (Calvo et al., 2007). Unfortunately the resolution and chronological control of the LM2 record were not sufficient to determine if the observed fluctuations in this MAAT record showed a similar cyclicity. The LM2 MAAT record during the late Holocene shows a different trend compared to cores GC-12 and GC-25 that showed general increase in temperature during this same period (Fig. 10). Higher water levels are reported at Lake Allom during this period, along with lower fire activity in the surrounding area (Donders et al., 2006), indicating that effective precipitation was higher than during the mid-Holocene.

Summary and conclusions

Quantitative reconstructions of climate in the southern hemisphere are rare and yet of high importance to further our understanding of climate change and associated biological responses. This study highlights the potential of using branched GDGT distributions as a proxy for the quantitative reconstruction of trends and amplitudes of past temperature variability from lacustrine sediment archives. The apparent accuracy of the branched GDGT temperature estimates at Lake McKenzie may be at least partially due to the predominantly allochthonous origin of branched GDGTs observed in the sediments of this lake. In many lake systems, the branched GDGTs observed in sediments are likely to derive from both allochthonous and autochthonous sources (eg Blaga et al., 2009; Tierney and Russell, 2009; Pearson et al., 2011; Sun et al., 2011), making these more complex systems to infer temperatures from branched GDGT relative to Lake McKenzie.

https://doi.org/10.1016/j.yqres.2014.02.005 Published online by Cambridge University Press

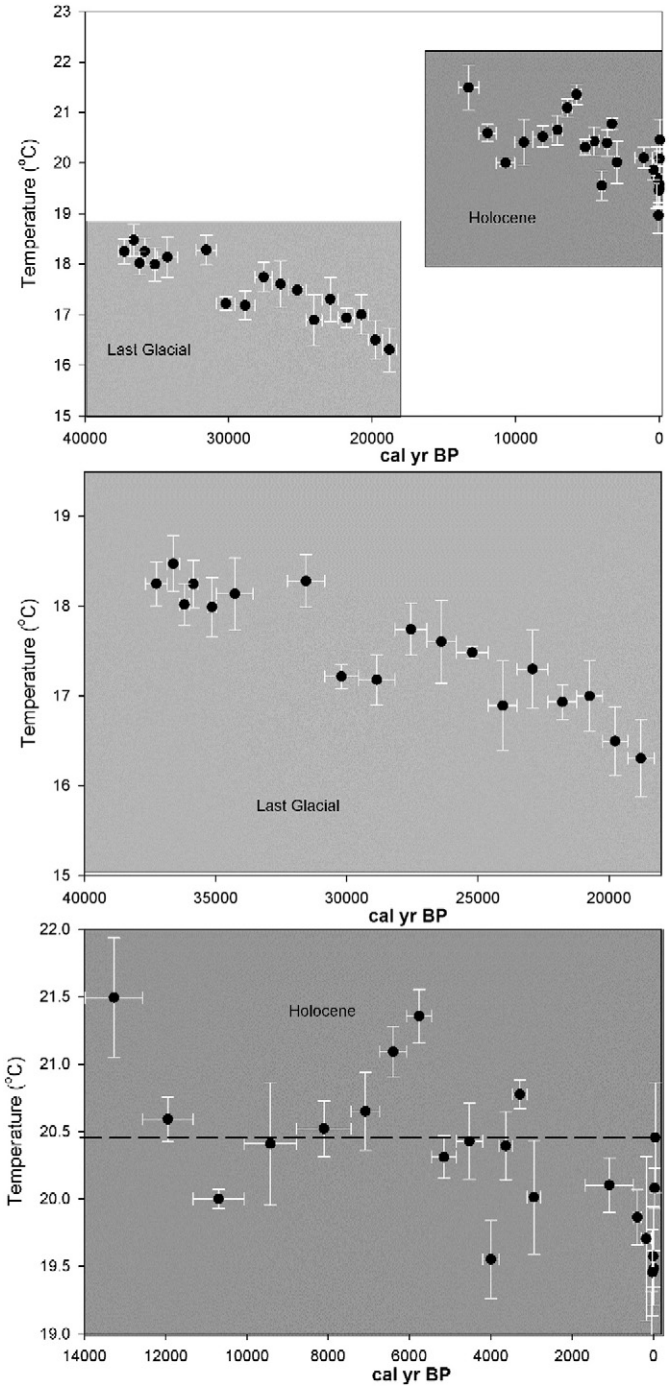

Figure 9. Lake McKenzie branched GDGT based inferred record of MAAT variability during both the end of the last Glacial period (light grey) and the Holocene (dark grey). The dashed line reflects the modern day MAAT of 20.4°C, as observed in the top 1 cm of sediment from Lake McKenzie. Horizontal error bars depict the upper and lower age estimates for each sample, while the vertical error bars reflect the standard deviation around the mean temperature estimate using at least triplicate or more measurements of each sample. *ages were interpolated from the age model, where zero means AD 1950.

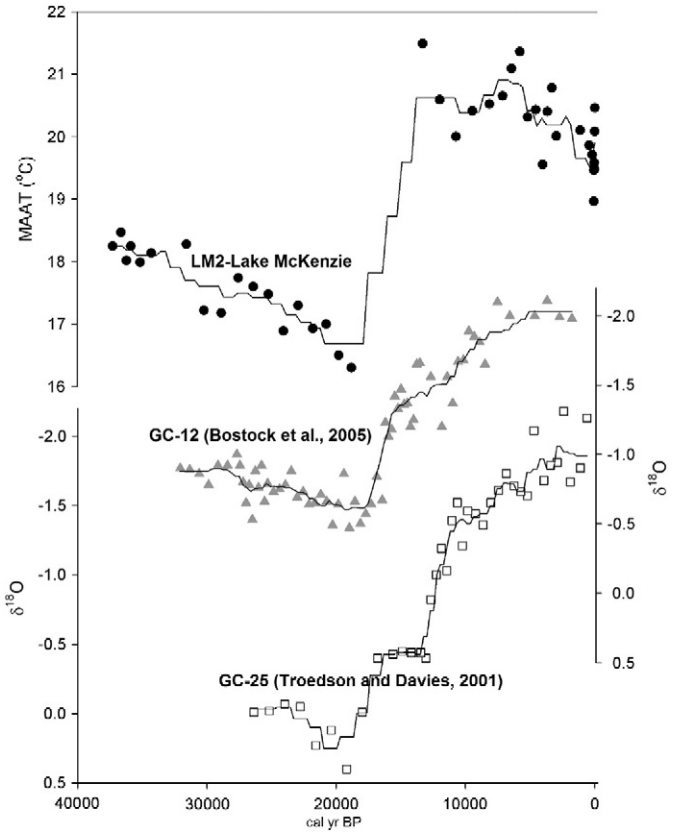

Figure 10. The Lake McKenzie MAAT record plotted together with two $\delta^{18}O$ of *G. ruber* marine records located north (GC-12, Bostock et al., 2005) and south (GC-25, Troedson and Davies, 2001) of Fraser Island. Lines through the points represent a three point running averages. *ages were interpolated from the age model, where zero means AD 1950.

The Lake McKenzie MAAT record presented in this study contributes to the relatively sparse array of quantitative information about temperature variability during the last glacial period on the Australian continent. The location, length, and apparent quantitative nature of the Lake McKenzie terrestrial MAAT reconstruction makes it well positioned for future paleoclimate model/data comparison studies that compare terrestrial and marine climate records to obtain new insight on the difference in response to the terrestrial climate relative to global climatic changes. This may be instrumental for constraining future projections of climate change on the Australian continent.

Acknowledgments

We thank: Sarah Hembrow, Linda Barry and Kerry Wilsher for their assistance with field work at Lake McKenzie. Additionally we give special thanks to Colin Lawton from the Queensland Parks and Wildlife Service for collecting and sending soil samples from the drainage basin of Lake McKenzie. Atun Zawadski, Jack Goralewski and Daniela Fierro are acknowledged for their work on the ^{210}Pb dating and Fiona Bertuch and Alan Williams are thanked for their assistance with the AMS ^{14}C dating. We additionally thank Prof Lorenz Schwark for the critical discussions about this research project.

Martijn Woltering and Kliti Grice were supported by an ARC QEII Discovery grant awarded to KG. Funding for the LC-MS Orbitrap facility at Curtin University was supplied by an ARC LIEFP grant, the WA-OIGC and the John de Laeter Centre for Isotope Research.

Appendix A. Supplementary data

Supplementary data to this article can be found online at http://dx.doi.org/10.1016/j.yqres.2014.02.005.

References

Abram, N.J., McGregor, H.V., Gagan, M.K., Hantoro, W.S., Suwargadi, B.W., 2009. Oscillations in the southern extent of the Indo-Pacific warm pool during the mid-Holocene. Quaternary Science Reviews 28, 2794–2803.

Appleby, P.G., 2001. Chronostratigraphic techniques in recent sediments. In: Last, W.M., Smol, J.P. (Eds.), Tracking Environmental Change Using Lake Sediments. Basin

Analysis, Coring and Chronological Techniques, 1. Kluwer Academic Publishers, Dordrecht, pp. 171–203.
Appleby, P.G., Oldfield, F., 1978. The calculation of lead-210 dates assuming a constant rate of supply of unsupported 210Pb to the sediment. Catena 5, 1–8.
Appleby, P.G., Oldfield, F., 1992. Application of ^{210}Pb to sediment studies. In: Ivonavich, M., Harmon, R.S. (Eds.), Uranium-Series disequilibrium: Applications to Earth, Marine and Environmental Science. Oxford University Press, Oxford, pp. 731–778.
Armand, L.K., Leventer, A., 2010. Palaeo sea ice distribution and reconstruction derived from the geological record. Sea Ice 469–530.
Australian Bureau of Meteorology (BOM), 2013. Australian Government 21/12/2013. http://www.bom.gov.au/.
Barrell, D.J.A., Almond, P.C., Vandergoes, M.J., Lowe, D.J., Newnham, R.M., 2013. A composite pollen-based stratotype for inter-regional evaluation of climatic events in New Zealand over the past 30,000 years (NZ-INTIMATE project). Quaternary Science Reviews 74, 4–20.
Barrows, T.T., Juggins, S., 2005. Sea-surface temperatures around the Australian margin and Indian Ocean during the Last Glacial Maximum. Quaternary Science Reviews 24, 1017–1047.
Barrows, T.T., Stone, J.O., Fifield, L.K., Cresswell, R.G., 2001. Late Pleistocene glaciation of the Kosciuszko Massif, Snowy Mountains, Australia. Quaternary Research 55, 179–189.
Barrows, T.T., Juggins, S., De Deckker, P., Calvo, E., Pelejero, C., 2007. Long-term sea surface temperature and climate change in the Australian–New Zealand region. Paleoceanography 22, PA2215.
Bechtel, A., Smittenberg, R.H., Bernasconi, S.M., Schubert, C.J., 2010. Distribution of branched and isoprenoid tetraether lipids in an oligotrophic and a eutrophic Swiss lake: insights into sources and GDGT-based proxies. Organic Geochemistry 41, 822–832.
Blaga, C.I., Reichart, G.J., Heiri, O., Sinninghe Damsté, J.S., 2009. Tetraether membrane lipid distributions in water-column particulate matter and sediments: a study of 47 European lakes along a north–south transect. Journal of Paleolimnology 41, 523–540.
Blunier, T., Brook, E.J., 2001. Timing of millennial-scale climate change in Antarctica and Greenland during the last glacial period. Science 291, 109–112.
Bostock, H.C., Opdyke, B.N., Gagan, M.K., Kiss, A.E., Fifield, L.K., 2006. Glacial/interglacial changes in the East Australian current. Climate Dynamics 26, 645–659.
Bowler, J.M., 1976. Aridity in Australia: age, origins and expression in aeolian landforms and sediments. Earth-Science Reviews 12, 279–310.
Bowler, J.M., Gillespie, R., Johnston, H., Boljkovac, K., 2012. Wind v water: glacial maximum records from the Willandra Lakes, 34. Terra Australis 271–296.
Bowling, L.C., 1988. Optical properties, nutrients and phytoplankton of freshwater coastal dune lakes in south-east Queensland. Australian Journal of Marine and Freshwater Research 39, 805–815.
Bronk Ramsey, C., 2009. Bayesian analysis of radiocarbon dates. Radiocarbon 51, 337–360.
Calvo, E., Pelejero, C., De Deckker, P., Logan, G.A., 2007. Antarctic deglacial pattern in a 30 kyr record of sea surface temperature offshore South Australia. Geophysical Research Letters 34, 1–6.
Clark, P.U., Dyke, A.S., Shakun, J.D., Carlson, A.E., Clark, J., Wohlfarth, B., Mitrovica, J.X., Hostetler, S.W., McCabe, A.M., 2009. The last glacial maximum. Science 325, 710–714.
Das, S.K., Bendle, J., Routh, J., 2012. Evaluating branched tetraether lipid-based palaeotemperature proxies in an urban, hyper-eutrophic polluted lake in South Africa. Organic Geochemistry 53, 45–51.
D'Costa, D.M., Edney, P., Kershaw, A.P., Deckker, P.D., 1989. Late Quaternary palaeoecology of Tower Hill, Victoria, Australia. Journal of Biogeography 16, 461–482.
De Deckker, P., Moros, M., Perner, K., Jansen, E., 2012. Influence of the tropics and southern westerlies on glacial interhemispheric asymmetry. Nature Geoscience 5, 266–269.
Denton, G.H., Lowell, T.V., Heusser, C.J., Moreno, P.I., Andersen, B.G., Heusser, L.E., Schlüchter, C., Marchant, D.R., 1999. Interhemispheric linkage of paleoclimate during the last glaciation. Geografiska Annaler. Series A Physical Geography 81, 107–153.
Donders, T.H., Wagner, F., Visscher, H., 2006. Late Pleistocene and Holocene subtropical vegetation dynamics recorded in perched lake deposits on Fraser Island, Queensland, Australia. Palaeogeography Palaeoclimatology Palaeoecology 241, 417–439.
EPICA Members, 2006. One-to-one coupling of glacial climate variability in Greenland and Antarctica. Nature 444, 195–198.
Fawcett, P.J., Werne, J.P., Anderson, R.S., Heikoop, J.M., Brown, E.T., Berke, M.A., Smith, S.J., Goff, F., Donohoo-Hurley, L., Cisneros-Dozal, L.M., Schouten, S., Damste, J.S.S., Huang, Y.S., Toney, J., Fessenden, J., WoldeGabriel, G., Atudorei, V., Geissman, J.W., Allen, C.D., 2011. Extended megadroughts in the southwestern United States during Pleistocene interglacials. Nature 470, 518–521.
Gagan, M.K., Ayliffe, L.K., Hopley, D., Cali, J.A., Mortimer, G.E., Chappell, J., McCulloch, M.T., Head, M.J., 1998. Temperature and surface-ocean water balance of the mid-Holocene Tropical Western Pacific. Science 279, 1014–1018.
Gagan, M.K., Hendy, E.J., Haberle, S.G., Hantoro, W.S., 2004. Post-glacial evolution of the Indo-Pacific Warm Pool and El Niño-Southern oscillation. Quaternary International 118–119, 127–143.
Hadwen, W.L., 2002. Effects of Nutrient Additions on Dune Lakes on Fraser Island, Australia, Faculty of Environmental Sciences. Griffith University, Brisbane.
Harrison, S.P., 1993. Late Quaternary lake-level changes and climates of Australia. Quaternary Science Reviews 12, 211–231.
Hellstrom, J., McCulloch, M., Stone, J., 1998. A detailed 31,000-year record of climate and vegetation change, from the isotope geochemistry of two New Zealand speleothems. Quaternary Research 50, 167–178.
Hembrow, S., Taffs, K., Atahan, P., Parr, J., Zawadzki, A., Heijnis, H., 2014. Diatom community response to climate variability over the past 37,000 years in the sub-tropics of the Southern Hemisphere. Science of the Total Environment 468–469, 774–784.
Hua, Q., Zoppi, U., Williams, A.A., Smith, A.M., 2004. Small-mass AMS radiocarbon analysis at ANTARES. Nuclear Instruments and Methods in Physics Research Section B: Beam Interactions with Materials and Atoms 223–224, 284–292.
World Heritage Nomination – IUCN technical Evaluation, 1992. 630 Fraser Island and the Great Sandy Region (Australia). Nature IUCN, Gland, Switzerland.
Kershaw, A.P., 1986. Climatic change and Aboriginal burning in north-east Australia during the last two glacial/interglacial cycles. Nature 322, 47–49.
Kershaw, A.P., Nanson, G.C., 1993. The last full glacial cycle in the australian region. Global and Planetary Change 7, 1–9.
Longmore, M.E., 1997. Quaternary palynological records from perched lake sediments, Fraser Island, Queensland, Australia: rainforest, forest history and climatic control. Australian Journal of Botany 45, 507–526.
Longmore, M.E., Heijnis, H., 1999. Aridity in Australia: Pleistocene records of palaeohydrological and palaeoecological change from the perched lake sediments of Fraser Island, Queensland, Australia. Quaternary International 57–8, 35–47.
Loomis, S.E., Russell, J.M., Sinninghe Damsté, J.S., 2011. Distributions of branched GDGTs in soils and lake sediments from western Uganda: implications for a lacustrine paleothermometer. Organic Geochemistry 42, 739–751.
Loomis, S.E., Russell, J.M., Ladd, B., Street-Perrott, F.A., Sinninghe Damsté, J.S., 2012. Calibration and application of the branched GDGT temperature proxy on East African lake sediments. Earth and Planetary Science Letters 357–358, 277–288.
McKenzie, N., Jacquier, D., Isbell, R., Brown, K., 2004. Australian Soils and Landscapes: An Illustrated Compendium. CSIRO Publishing, Collingwood, Australia.
Miller, G.H., Magee, J.W., Jull, A.J.T., 1997. Low-latitude glacial cooling in the Southern Hemisphere from amino-acid racemization in emu eggshells. Nature 385, 241–244.
Moss, P.T., Kershaw, A.P., 2000. The last glacial cycle from the humid tropics of northeastern Australia: comparison of a terrestrial and a marine record. Palaeogeography Palaeoclimatology Palaeoecology 155, 155–176.
Moss, P.T., Kershaw, A.P., 2007. A late Quaternary marine palynological record (oxygen isotope stages 1 to 7) for the humid tropics of northeastern Australia based on ODP Site 820. Palaeogeography Palaeoclimatology Palaeoecology 251, 4–22.
Niemann, H., Stadnitskaia, A., Wirth, S.B., Gilli, A., Anselmetti, F.S., Sinninghe Damsté, J.S., Schouten, S., Hopmans, E.C., Lehmann, M.F., 2012. Bacterial GDGTs in Holocene sediments and catchment soils of a high Alpine lake: application of the MBT/CBT-paleothermometer. Climate of the Past 8, 889–906.
Pearson, E.J., Juggins, S., Talbot, H.M., Weckstrom, J., Rosen, P., Ryves, D.B., Roberts, S.J., Schmidt, R., 2011. A lacustrine GDGT-temperature calibration from the Scandinavian Arctic to Antarctic: renewed potential for the application of GDGT-paleothermometry in lakes. Geochimica et Cosmochimica Acta 75, 6225–6238.
Peterse, F., Prins, M.A., Beets, C.J., Troelstra, S.R., Zheng, H., Gu, Z., Schouten, S., Damsté, J.S.S., 2011. Decoupled warming and monsoon precipitation in East Asia over the last deglaciation. Earth and Planetary Science Letters 301, 256–264.
Peterse, F., van der Meer, J., Schouten, S., Weijers, J.W.H., Fierer, N., Jackson, R.B., Kim, J.H., Sinninghe Damsté, J.S., 2012. Revised calibration of the MBT-CBT paleotemperature proxy based on branched tetraether membrane lipids in surface soils. Geochimica et Cosmochimica Acta 96, 215–219.
Petherick, L., Bostock, H., Cohen, T.J., Fitzsimmons, K., Tibby, J., Fletcher, M.S., Moss, P., Reeves, J., Mooney, S., Barrows, T., 2013. Climatic records over the past 30 ka from temperate Australia—a synthesis from the Oz-INTIMATE workgroup. Quaternary Science Reviews 74, 58–77.
Pickett, E.J., Harrison, S.P., Hope, G., Harle, K., Dodson, J.R., Peter Kershaw, A., Colin Prentice, I., Backhouse, J., Colhoun, E.A., D'Costa, D., Flenley, J., Grindrod, J., Haberle, S., Hassell, C., Kenyon, C., Macphail, M., Martin, H., Martin, A.H., McKenzie, M., Newsome, J.C., Penny, D., Powell, J., Ian Raine, J., Southern, W., Stevenson, J., Sutra, J.-P., Thomas, I., van der Kaars, S., Ward, J., 2004. Pollen-based reconstructions of biome distributions for Australia, Southeast Asia and the Pacific (SEAPAC region) at 0, 6000 and 18,000 14C yr BP. Journal of Biogeography 31, 1381–1444.
Reeves, J.M., Bostock, H.C., Ayliffe, L.K., Barrows, T.T., De Deckker, P., Devriendt, L.S., Dunbar, G.B., Drysdale, R.N., Fitzsimmons, K.E., Gagan, M.K., 2013. Palaeoenvironmental change in tropical Australasia over the last 30,000 years—a synthesis by the OZ-INTIMATE group. Quaternary Science Reviews 97–114.
Reimer, P.J., Baillie, M.G.L., Bard, E., Bayliss, A., Beck, J.W., Blackwell, P.G., Ramsey, C.B., Buck, C.E., Burr, G.S., Edwards, R.L., Friedrich, M., Grootes, P.M., Guilderson, T.P., Hajdas, I., Heaton, T.J., Hogg, A.G., Hughen, K.A., Kaiser, K.F., Kromer, B., McCormac, F.G., Manning, S.W., Reimer, R.W., Richards, D.A., Southon, J.R., Talamo, S., Turney, C.S.M., van der Plicht, J., Weyhenmeye, C.E., 2009. Intcal09 and marine09 radiocarbon age calibration curves, 0–50,000 years cal bp. Radiocarbon 51, 1111–1150.
Rueda, G., Rosell-Mele, A., Escala, M., Gyllencreutz, R., Backman, J., 2009. Comparison of instrumental and GDGT-based estimates of sea surface and air temperatures from the Skagerrak. Organic Geochemistry 40, 287–291.
Shakun, J.D., Clark, P.U., He, F., Marcott, S.A., Mix, A.C., Liu, Z., Otto-Bliesner, B., Schmittner, A., Bard, E., 2012. Global warming preceded by increasing carbon dioxide concentrations during the last deglaciation. Nature 484, 49–54.
Sinninghe Damsté, J.S., Hopmans, E.C., Pancost, R.D., Schouten, S., Geenevasen, J.A.J., 2000. Newly discovered non-isoprenoid glycerol dialkyl glycerol tetraether lipids in sediments. Chemical Communications 1683–1684.
Sinninghe Damsté, J.S., Ossebaar, J., Abbas, B., Schouten, S., Verschuren, D., 2009. Fluxes and distribution of tetraether lipids in an equatorial African lake: constraints on the application of the TEX86 palaeothermometer and BIT index in lacustrine settings. Geochimica et Cosmochimica Acta 73, 4232–4249.
Sinninghe Damsté, J.S., Ossebaar, J., Schouten, S., Verschuren, D., 2012. Distribution of tetraether lipids in the 25-ka sedimentary record of Lake Challa: extracting reliable TEX86 and MBT/CBT palaeotemperatures from an equatorial African lake. Quaternary Science Reviews 50, 43–54.
Suggate, R.P., 1990. Late pliocene and quaternary glaciations of New Zealand. Quaternary Science Reviews 9, 175–197.
Sun, Q., Chu, G.Q., Liu, M.M., Xie, M.M., Li, S.Q., Ling, Y.A., Wang, X.H., Shi, L.M., Jia, G.D., Lu, H.Y., 2011. Distributions and temperature dependence of branched glycerol dialkyl

https://doi.org/10.1016/j.yqres.2014.02.005 Published online by Cambridge University Press

glycerol tetraethers in recent lacustrine sediments from China and Nepal. Journal of Geophysical Research-Biogeosciences 116.
Tierney, J.E., Russell, J.M., 2009. Distributions of branched GDGTs in a tropical lake system: implications for lacustrine application of the MBT/CBT paleoproxy. Organic Geochemistry 40, 1032–1036.
Tierney, J.E., Russell, J.M., Huang, Y.S., Sinninghe Damsté, J.S., Hopmans, E.C., Cohen, A.S., 2008. Northern hemisphere controls on tropical southeast African climate during the past 60,000 years. Science 322, 252–255.
Tierney, J.E., Russell, J.M., Eggermont, H., Hopmans, E.C., Verschuren, D., Sinninghe Damsté, J.S., 2010. Environmental controls on branched tetraether lipid distributions in tropical East African lake sediments. Geochimica et Cosmochimica Acta 74, 4902–4918.
Tierney, J.E., Schouten, S., Pitcher, A., Hopmans, E.C., Sinninghe Damsté, J.S., 2012. Core and intact polar glycerol dialkyl glycerol tetraethers (GDGTs) in Sand Pond, Warwick, Rhode Island (USA): insights into the origin of lacustrine GDGTs. Geochimica et Cosmochimica Acta 77, 561–581.
Troedson, A.L., Davies, P.J., 2001. Contrasting facies patterns in subtropical and temperate continental slope sediments: inferences from east Australian late Quaternary records. Marine Geology 172, 265–285.
Turney, C.S.M., Kershaw, A.P., James, S., Branch, N., Cowley, J., Fifield, L.K., Jacobsen, G., Moss, P., 2006. Geochemical changes recorded in Lynch's Crater, Northeastern Australia, over the past 50 ka. Palaeogeography, Palaeoclimatology, Palaeoecology 233, 187–203.
Tyler, J.J., Nederbragt, A.J., Jones, V.J., Thurow, J.W., 2010. Assessing past temperature and soil pH estimates from bacterial tetraether membrane lipids: evidence from the recent lake sediments of Lochnagar, Scotland. Journal of Geophysical Research-Biogeosciences 115, G001109.
Vandergoes, M.J., Newnham, R.M., Preusser, F., Hendy, C.H., Lowell, T.V., Fitzsimons, S.J., Hogg, A.G., Kasper, H.U., Schluchter, C., 2005. Regional insolation forcing of late Quaternary climate change in the Southern Hemisphere. Nature 436, 242–245.
Webb, T., 1986. Is vegetation in equilibrium with climate? How to interpret late-Quaternary pollen data. Plant Ecology 67, 75–91.
Weijers, J.W.H., Schouten, S., Hopmans, E.C., Geenevasen, J.A.J., David, O.R.P., Coleman, J.M., Pancost, R.D., Sinninghe Damsté, J.S., 2006. Membrane lipids of mesophilic anaerobic bacteria thriving in peats have typical archaeal traits. Environmental Microbiology 8, 648–657.
Weijers, J.W.H., Schefuss, E., Schouten, S., Sinninghe Damsté, J.S., 2007a. Coupled thermal and hydrological evolution of tropical Africa over the last deglaciation. Science 315, 1701–1704.
Weijers, J.W.H., Schouten, S., van den Donker, J.C., Hopmans, E.C., Sinninghe Damsté, J.S., 2007b. Environmental controls on bacterial tetraether membrane lipid distribution in soils. Geochimica et Cosmochimica Acta 71, 703–713.
Woltering, M., Johnson, T.C., Werne, J.P., Schouten, S., Sinninghe Damsté, J.S., 2011. Late Pleistocene temperature history of Southeast Africa: a TEX86 temperature record from Lake Malawi. Palaeogeography Palaeoclimatology Palaeoecology 303, 93–102.
Zink, K.-G., Vandergoes, M.J., Mangelsdorf, K., Dieffenbacher-Krall, A.C., Schwark, L., 2010. Application of bacterial glycerol dialkyl glycerol tetraethers (GDGTs) to develop modern and past temperature estimates from New Zealand lakes. Organic Geochemistry 41, 1060–1066.

https://doi.org/10.1016/j.yqres.2014.02.005 Published online by Cambridge University Press